SURFACE CHEMISTRY

Following the microscopic pathway to adsorption through chemisorption and physisorption wells

Dmitriy Borodin[1,2], Igor Rahinov[3], Pranav R. Shirhatti[4], Meng Huang[5], Alexander Kandratsenka[2], Daniel J. Auerbach[2], Tianli Zhong[1,2], Hua Guo[5], Dirk Schwarzer[2], Theofanis N. Kitsopoulos[1,2,6,7], Alec M. Wodtke[1,2,8]*

Adsorption involves molecules colliding at the surface of a solid and losing their incidence energy by traversing a dynamical pathway to equilibrium. The interactions responsible for energy loss generally include both chemical bond formation (chemisorption) and nonbonding interactions (physisorption). In this work, we present experiments that revealed a quantitative energy landscape and the microscopic pathways underlying a molecule's equilibration with a surface in a prototypical system: CO adsorption on Au(111). Although the minimum energy state was physisorbed, initial capture of the gas-phase molecule, dosed with an energetic molecular beam, was into a metastable chemisorption state. Subsequent thermal decay of the chemisorbed state led molecules to the physisorption minimum. We found, through detailed balance, that thermal adsorption into both binding states was important at all temperatures.

Adsorption of molecules to metal surfaces initiates most heterogeneous chemistry; yet, the precise way it occurs is difficult to study. When hot molecules collide with a surface, they must lose translational and internal energy, ultimately reaching equilibrium with the solid. This process may involve forming transient chemical bonds to the surface, leading to chemisorption (*1*) or, alternatively, noncovalent (physisorption) interactions. Furthermore, which interactions prevail can strongly influence surface chemistry (*2*, *3*); for example, chemisorbed O_2 on Pt(111) can dissociate producing highly reactive adsorbed atoms (*4*), whereas physisorbed O_2 desorbs, remaining unreactive (*5*).

Generally, molecules adsorb through both physisorption and chemisorption interactions (*5*). Hence, adsorption generally involves passage through multiple binding states before equilibrium is achieved. This process represents a complex and fundamental problem that is not well understood. For example, one might think that physisorption is more important for accommodation of impinging molecules. For the CO/Au(111) system, density functional theory (DFT) calculations suggest that when chemisorbed, CO binds with a fixed (OC-Au) orientation and at specific sites; but when physisorbed, CO is nearly a free rotor and weakly bound at every surface site (*6*). When a molecule collides randomly at different surface sites and with random orientation, physisorption is statistically favored. But this scenario ignores that rates of equilibration depend strongly on the nature of the interactions. For example, the vibrational relaxation time of chemisorbed CO to Cu is ~2 ps (*7*) but is 49 ps for CO physisorbed to Au (*8*).

The intricate interplay between physisorption and chemisorption states is believed to take place in precursor-mediated adsorption (*9*–*11*) and bear on a broad variety of surface science applications, ranging from catalytic steam reforming (*10*, *11*) to designing molecular switches (*12*). Despite being central to a dynamical picture of surface chemistry, predicting and probing adsorption pathways exceeds our current understanding. Not only is electronic structure theory challenged to provide accurate, simultaneous descriptions of covalent and noncovalent interactions, but also no experiments so far have been reported that directly follow adsorption pathways through chemisorption and physisorption wells. Recently, we observed that vibrationally excited CO can trap to a gold surface, equilibrating

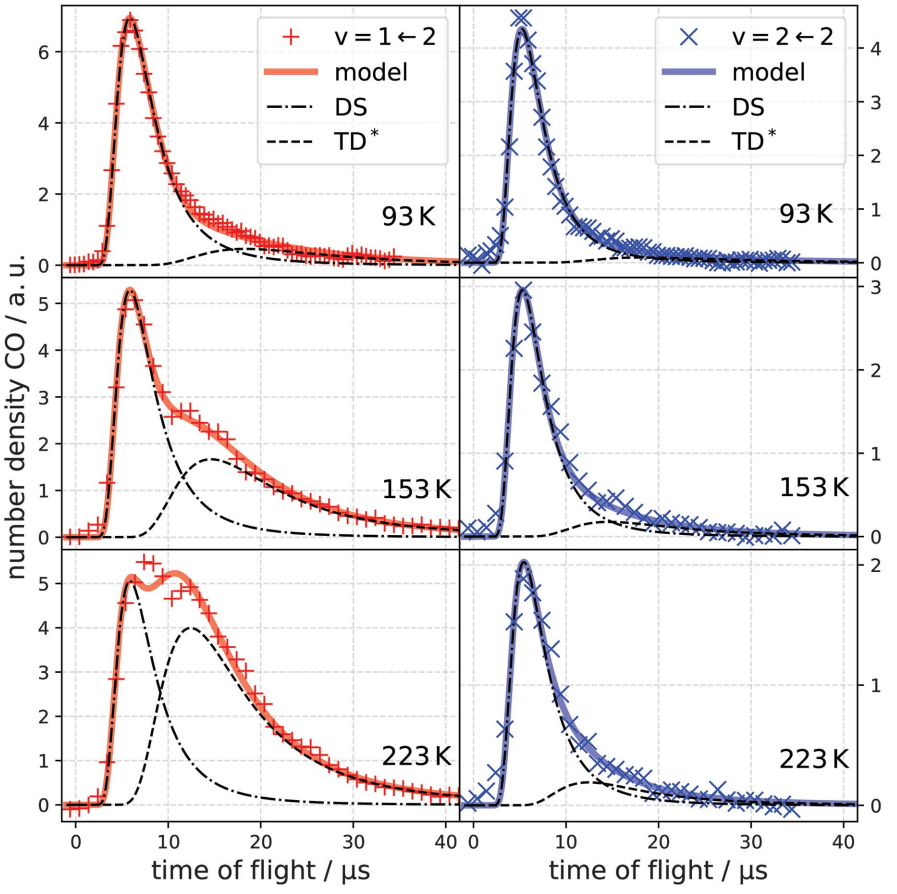

Fig. 1. State-specific time of flight traces. Measured TOF traces of CO(v = 1) (+ symbols) and CO(v = 2) (× symbols) at different surface temperatures along with their global fits (solid lines) revealing the DS (dash-dotted lines) and TD* (dashed lines) components. The incidence energy is E_i = 0.32 eV. The surface temperature is indicated in each panel. The method for decomposing the data into DS and TD* components is explained in the supplementary materials, section 1.

[1]Institute for Physical Chemistry, Georg-August University of Göttingen, Tammannstraße 6, 37077 Göttingen, Germany. [2]Department of Dynamics at Surfaces, Max Planck Institute for Biophysical Chemistry, Am Faßberg 11, 37077 Göttingen, Germany. [3]Department of Natural Sciences, The Open University of Israel, 4353701 Raanana, Israel. [4]Tata Institute of Fundamental Research, 500046 Hyderabad, India. [5]Department of Chemistry and Chemical Biology, University of New Mexico, Albuquerque, NM 87131, USA. [6]Department of Chemistry, University of Crete, 71003 Heraklion, Greece. [7]Institute of Electronic Structure and Laser, FORTH, 71110 Heraklion, Greece. [8]International Center for Advanced Studies of Energy Conversion, Georg-August University of Göttingen, Tammannstraße 6, 37077 Göttingen, Germany.
*Corresponding author. Email: alec.wodtke@mpibpc.mpg.de

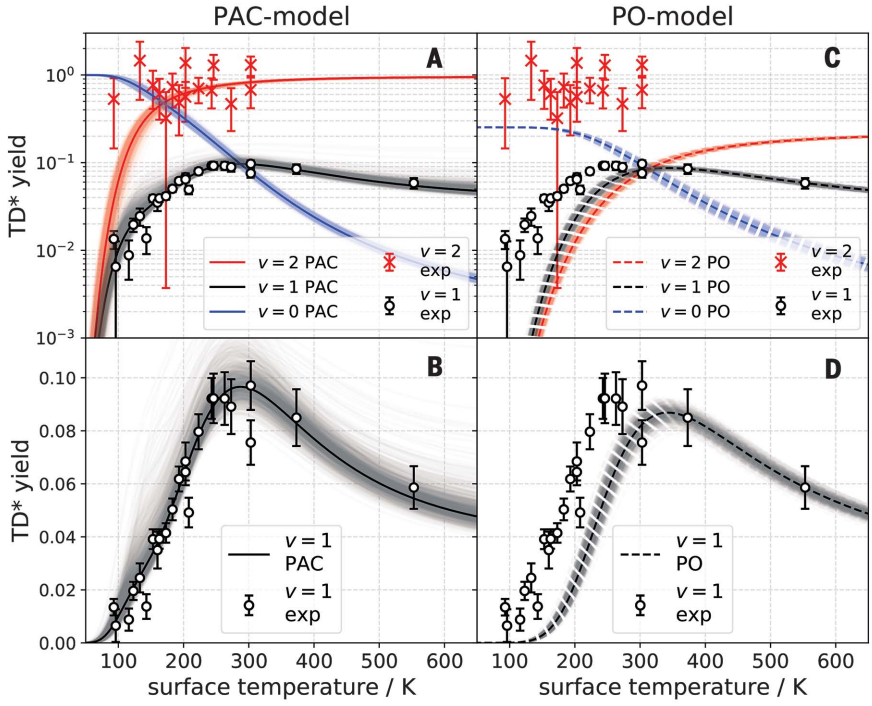

Fig. 2. Vibrational state–specific yields of desorbing molecules. (**A** to **D**) Experimentally observed CO(v = 1) (open circles) and CO(v = 2) (× symbols) passing through the TD* channel. The error bars indicate a 90% confidence interval. Black and red solid lines are results of fits to the PAC model. (A) Logarithmic scale. (B), Linear scale. Black and red dashed lines represent the PO model. (C) Logarithmic scale. (D) Linear scale. Blue solid line (PAC) and blue dashed line (PO) represent the desorbing yield of CO(v = 0) stemming from ultimate vibrational relaxation of CO(v = 2). The shading represents the uncertainty of the fit determined by random number sampling of the fit parameter distribution (supplementary materials, section 4).

both its rotational and translational motion but without vibrational equilibration (*13*). As we will show below, this feature provided a distinctive opportunity to follow the microscopic pathways of adsorption and equilibration on the surface, using the vibrational relaxation time as an internal clock.

Specifically, we have demonstrated that the adsorption of energetic CO to Au(111) involves pathways through a chemisorption state recently predicted by theory (*6*) as well as the known physisorption state (*8*, *14*). We showed that although the overall free-energy minimum is the physisorbed state, when an energized molecule collides with the surface, it first becomes trapped in a metastable chemisorption state, in which it rapidly loses its vibrational and translational energy to the solid. We were able to derive the adsorption energies of the two states and the height of the energy barrier separating them. Application of the principle of detailed balance allowed us to use the information obtained in this molecular beam experiment to probe the pathway to thermal adsorption. This analysis showed that thermal adsorption involves substantial contributions from both chemisorption and physisorption at all temperatures.

The experiment involved scattering a molecular beam of optically prepared CO($v = 2, J = 1$) from Au(111) (where v is a vibrational quantum number and J is a rotational quantum number) and state-selectively detecting, at controlled surface temperature (T_S), the time of flight (TOF) of the thermally desorbing molecules in v = 1 and v = 2, in addition to directly scattered ones (supplementary materials, materials and methods) (*13*). We were inspired by recent theoretical predictions of a metastable chemisorption state with a short vibrational relaxation lifetime (*6*). We knew that the physisorbed molecule undergoes slow vibrational relaxation (*8*, *15*). So, it was clear that by varying T_S and thereby controlling the molecule's surface residence time, the

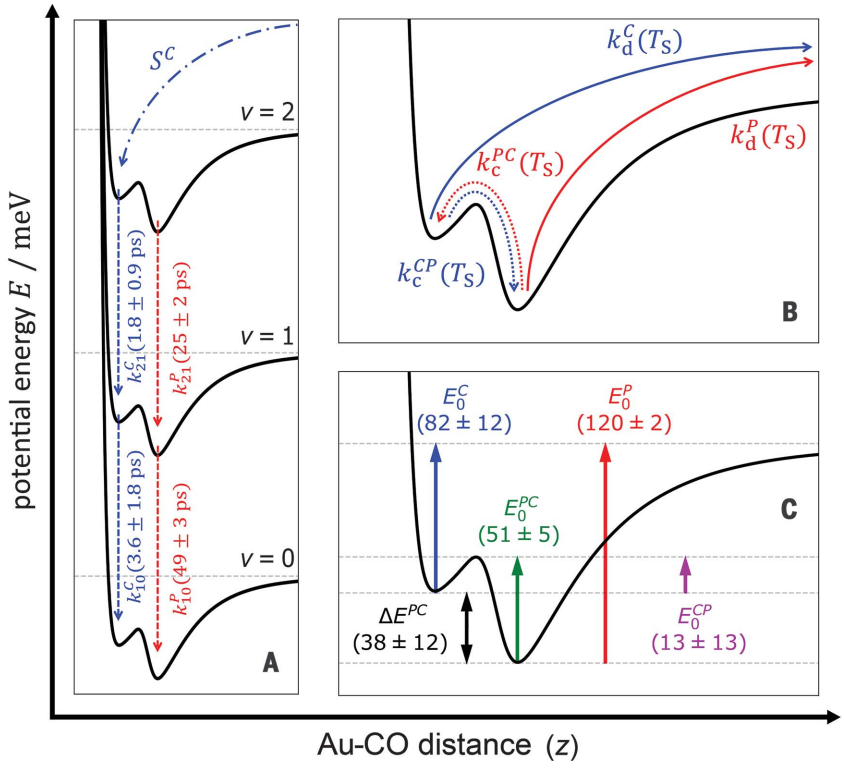

Fig. 3. The PAC model. (**A** and **B**) Rate processes describing the competition between (A) vibrational relaxation (dashed arrows) and (B) desorption (solid arrows) and interconversion between the chemisorbed and physisorbed states (dotted arrows). (**C**) Features of the Au(111)-CO interaction potential, derived from a fit of the PAC model to the experimental data.

temperature-independent vibrational relaxation lifetime could act as an internal clock, sensitive to the type of interaction that the molecule had experienced at the surface. Our goal was to obtain quantitative insight into the pathways to adsorption from measured populations of thermally desorbing CO in v = 1 and 2, which depend on the branching ratio between vibrational relaxation and desorption.

Examples of these TOF experiments are shown in Fig. 1. The traces comprise a high-speed direct scattering (DS) component and a slower component owing to thermal desorption (TD*) of CO(v = 1 or 2). We use the notation TD* to indicate that the vibrational relaxation is not complete despite all other degrees of freedom (rotation and translation) being thermalized with the surface (*13*).

We fit data such as that of Fig. 1 to a simple model on the basis of the principle of detailed balance (supplementary materials, section 1). Hence, the fitting also yields the sticking probability versus incidence kinetic energy for CO on Au(111), which agrees well with a previous report (*16*). This procedure also yielded vibrational state–specific populations of desorbing molecules in the TD* channel (Fig. 2). CO (v = 2) (Fig. 2, × symbols) dominated the TD* channel, but some CO also desorbed in v = 1 (Fig. 2, open circles). Desorption yield varied strongly with T_S and can be fit with a kinetic model involving physisorption and chemisorption states (PAC model).

The PAC model is shown schematically in Fig. 3, A and B, and is described further in the supplementary materials, section 2. The important rate processes are thermal desorption from the chemisorbed (k_d^C) and physisorbed (k_d^P) states; thermal conversion between the two states (k_c^{PC} and k_c^{CP}); and vibrational relaxation of chemisorbed (k_{ij}^C) and physisorbed (k_{ij}^P) molecules. Here, i and j are vibrational quantum numbers.

We have fit the vibrational state–specific quantities of Fig. 2, the × symbols and open circles, to the PAC model, optimizing only five parameters: k_{10}^C, the relaxation rate constant of chemisorbed CO(v = 1); ΔE^{PC}, the energy of the chemisorbed state relative to the physisorbed state; E_0^{PC}, the barrier to convert physisorbed molecules to the chemisorbed state; $A_c^{PC}(T_S)$, the Arrhenius prefactor to convert physisorbed molecules to the chemisorbed state; and S^C, the fraction of CO(v = 2) molecules that initially trap into the chemisorbed state. The values of parameters that result from the fits are provided in table S4.

Other constants in the model are known independently from temperature-programmed desorption (TPD) (*17*) or pump-probe measurements of vibrational lifetimes (*8*) or can be derived with the help of first-principles electronic structure calculations (*6*) and transition state theory (supplementary materials, section 3) (*18*–*20*).

The best fit is shown in Fig. 2, A and B, as black and red lines; all of the relevant rate constants are tabulated in the supplementary materials, section 3. A host of useful information emerges from the fitting. The derived energy landscape for adsorption is shown in Fig. 3C; this includes an analysis of TPD data yielding E_0^P, the desorption barrier from the physisorbed state (supplementary materials, section 3). We emphasize that S^C = 0.98 ± 0.02, indicating nearly exclusive initial population of the metastable chemisorption well in the molecular beam experiment and that molecules initially trapped in the chemisorbed state need only pass over a small barrier (of E_0^{CP} = 13 meV) to reach the physisorbed state, which is qualitatively consistent with predictions of first-principles electronic structure theory (*6*).

We also attempted to fit our results to models that neglect the chemisorption state (supplementary materials, section 5). In a physisorption-only (PO) model, adsorption occurs into a single physisorption well, and vibrational relaxation competes with thermal desorption. The PO model (Fig. 2, C and D, dashed black and red lines) failed to reproduce the experimental observations. Thermal desorption from the physisorbed state was much slower than from the chemisorbed state ($k_d^P \ll k_d^C$) (table S3); therefore, vibrationally excited molecules that were physisorbed relaxed more rapidly than they desorbed. This is mainly due to adsorbate entropy; the physisorbed state has the high entropy of a two-dimensional ideal gas, and the chemisorbed state has the low entropy of a hindered translator. By contrast, in the PAC model, rapid thermal desorption from the chemisorption well allowed CO (v = 2) to survive, which is in agreement with experiment. We also tried a third model that was based on the hypothesis that vibrational relaxation from v = 2 → 1 occurred during the subpicosecond interaction time of a DS event and that a fraction of these nascent CO(v = 1) molecules became trapped in the physisorption well (supplementary materials, section 5). This model also fails to describe the experimental observations.

The PAC model was supported by first-principles predictions of the coexistence of chemisorbed and physisorbed states (*6*). The precise energies of these states, the height of the energy barrier separating them, and the predicted vibrational relaxation lifetimes all depend on the specific assumptions of the theory and the chosen functional. Nevertheless, they were consistent with the experimentally derived values (supplementary materials, section 6).

Calculated microscopic pathway fluxes obtained from the experimentally validated PAC model are shown in Fig. 4. This includes pathways leading to CO(v = 1) desorption (Fig. 4A) and adsorption to the lowest energy physisorption minimum (Fig. 4B). Details on how pathway fluxes were determined are provided in the supplementary materials, section 7. At all temperatures, the first step toward equilibrium involved trapping of CO(v = 2) into the chemisorption well. This state can then undergo vibrational relaxation, thermal

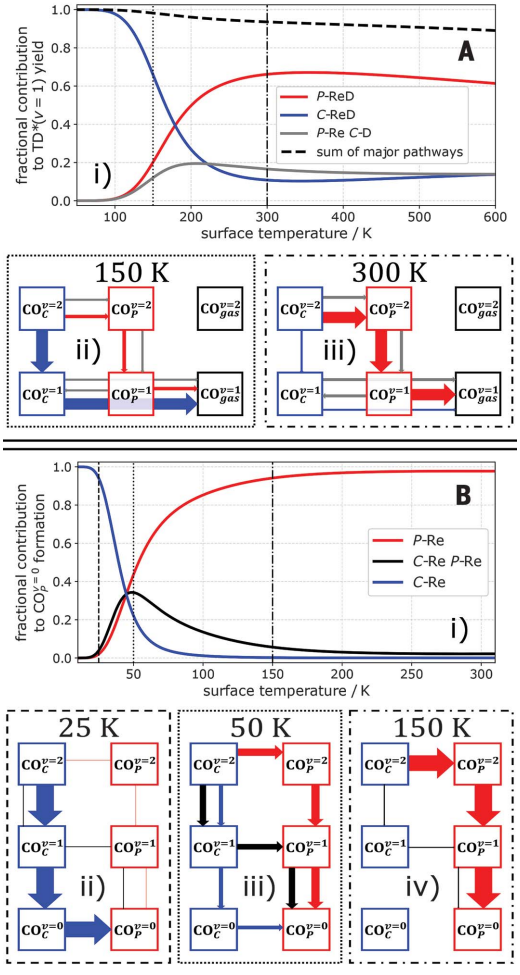

Fig. 4. Pathway fluxes for adsorption and desorption. (**A**) (Top) (i) Relative contribution of the most prominent pathways to CO(v = 1) desorption flux. (Bottom) Schematics illustrating the relative contributions of three most prominent pathways at (ii) low (150 K) and (iii) high (300 K) surface temperatures. (**B**) (Top) (i) Relative contribution of most prominent pathways of CO(v = 2) ultimate relaxation and formation of physisorbed CO(v = 0) on the surface. (Bottom) (ii to iv) Schematic representations of the most prominent pathways at different surface temperature regimes. The arrow thickness is proportional to the relative importance of the formation pathways.

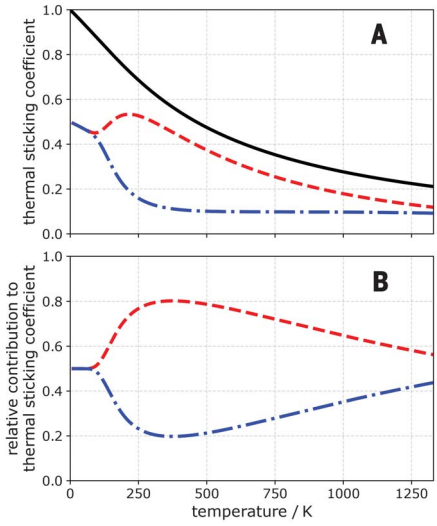

Fig. 5. Thermal adsorption into chemisorbed and physisorbed states. (**A**) Thermal sticking coefficients. (**B**) Relative contributions. Colored lines denote thermal adsorption into the physisorption (dashed, red) and chemisorption (dash-dotted, blue) wells. The black line is the total thermal adsorption coefficient.

desorption, and/or thermal conversion to the physisorbed state. At low temperatures (Fig. 4, blue lines and blue arrows), vibrational relaxation dominated because it required no thermal activation. At high temperature (Fig. 4, red lines and red arrows), conversion to the physisorbed species was rapid, followed by either desorption or vibrational relaxation. At intermediate temperatures, the physisorbed state could even transfer back to the chemisorption well.

Although the observations of these experiments are specific to vibrationally inelastic pathways to adsorption, the conclusions of this work are not. Vibrational motion has little influence on adsorption (*21*), and by applying the principle of detailed balance (supplementary materials, section 8) we can use the quantities derived from these molecular beam experiments to better understand thermal adsorption of CO to Au(111). Key results are shown in Fig. 5.

Thermal adsorption occurred initially into both the chemisorbed and physisorbed states, with similar probabilities at all temperatures. At low temperatures, adsorption into the two states was equally important. At intermediate temperatures, the higher-entropy physisorbed state increased in relative importance. But at the highest surface temperatures, the translational and rotational entropy of the chemisorbed CO approached that of the physisorbed CO and the chemisorbed CO again grew in importance. This increased entropy of the chemisorbed CO resulted from a greater sampling of higher-energy chemisorption states at different binding sites of the surface.

We also reconcile in Fig. 5 the seemingly contradictory observations that the molecular beam experiments exclusively probed the chemisorption state, but low-temperature thermal dosing experiments have never shown evidence of the chemisorption state (*8*, *14*). In the molecular beam experiments that used high-energy CO, the chemisorption state could be initially and selectively populated; these states were the same ones that became increasingly important in the high temperature range shown in Fig. 5. The high-temperature thermal adsorption still populated both states because of the large width of the Maxwell-Boltzmann distribution, while the width of the energy distribution in the molecular beam was orders of magnitude narrower (supplementary materials, section 8). For low-temperature dosing, it is clear now that both binding states were initially populated. But when we consider the small barrier to interconversion, it turns out that experiments have never been done at low enough temperatures to suppress thermal interconversion of the chemisorption to the physisorption state (supplementary materials, section 9). This analysis suggests an interesting experiment that could be carried out in the future. If a molecular beam with 0.3 eV incidence energy is used to selectively populate the chemisorption state and the surface is cooled below 5 K, it may be possible to suppress interconversion to the physisorbed state long enough to observe directly the metastable chemisorbed state.

Last, we highlight the implications of our work within the context of an industrially important class of catalytic reactions. Catalytic oxidation is initiated on a variety of metals through the reaction $O_{2(g)} \rightarrow O_2^*$, where O_2^* can be either physisorbed or chemisorbed. Hence, catalytic activation of oxygen, similar to many other examples in heterogeneous catalysis, is a complex network of thermal rate processes that includes adsorption into, desorption from, and interconversion between physisorbed and chemisorbed molecular states (*5*). Although these qualitative statements are long established, it has never before been possible to construct a model that accurately describes such a kinetic adsorption network. As a result, there has also never been a way to test to what extent theory is capable of describing such an intricately balanced set of rate processes. With the results presented here, we successfully determined the rate constants of a thermal adsorption network, revealing the fundamental energetic and entropic characteristics of adsorption and desorption. We also showed that the results can be understood from first principles by comparison with a multidimensional potential energy surface constructed with DFT (*6*). This result strengthens the foundation on which a predictive theory of surface chemistry and heterogeneous catalysis may continue to be developed.

REFERENCES AND NOTES

1. H. Jiang *et al.*, *Science* **364**, 379–382 (2019).
2. D. A. King, M. G. Wells, *Surf. Sci.* **29**, 454–482 (1972).
3. D. A. King, M. G. Wells, *Proc. R. Soc. London Ser. A* **339**, 245–269 (1974).
4. T. Zambelli, J. V. Barth, J. Wintterlin, G. Ertl, *Nature* **390**, 495–497 (1997).
5. C. T. Rettner, C. B. Mullins, *J. Chem. Phys.* **94**, 1626–1635 (1991).
6. M. Huang *et al.*, *Phys. Rev. B* **100**, 201407 (2019).
7. M. Morin, N. J. Levinos, A. L. Harris, *J. Chem. Phys.* **96**, 3950–3956 (1992).
8. S. Kumar *et al.*, *Phys. Rev. Lett.* **123**, 156101 (2019).
9. D. E. Brown, D. J. Moffatt, R. A. Wolkow, *Science* **279**, 542–544 (1998).
10. E. Dombrowski, E. Peterson, D. Del Sesto, A. L. Utz, *Catal. Today* **244**, 10–18 (2015).
11. R. Moiraghi *et al.*, *J. Phys. Chem. Lett.* **11**, 2211–2218 (2020).
12. W. Liu, S. N. Filimonov, J. Carrasco, A. Tkatchenko, *Nat. Commun.* **4**, 2569 (2013).
13. P. R. Shirhatti *et al.*, *Nat. Chem.* **10**, 592–598 (2018).
14. J. Pischel, A. Pucci, *J. Phys. Chem. C* **119**, 18340–18351 (2015).
15. I. Lončarić, M. Alducin, J. I. Juaristi, D. Novko, *J. Phys. Chem. Lett.* **10**, 1043–1047 (2019).
16. C. T. Rettner, *J. Chem. Phys.* **99**, 5481–5489 (1993).
17. D. P. Engelhart, R. J. V. Wagner, A. Meling, A. M. Wodtke, T. Schäfer, *Surf. Sci.* **650**, 11–16 (2016).
18. J. C. Tully, *Surf. Sci.* **299-300**, 667–677 (1994).
19. T. L. Hill, *Introduction to Statistical Thermodynamics* (Dover Publication, 1986).
20. M. Jørgensen, H. Grönbeck, *J. Phys. Chem. C* **121**, 7199–7207 (2017).
21. A. M. Wodtke, H. Yuhui, D. J. Auerbach, *Chem. Phys. Lett.* **413**, 326–330 (2005).
22. D. Borodin, CO(v=2) scattering on Au(111) (TPD, TOF and TD*(v=1,2)). Zenodo (2020).

ACKNOWLEDGMENTS

Funding: A.M.W. acknowledges support from the SFB1073 under project A04, from the Deutsche Forschungsgemeinschaft (DFG), and financial support from the Ministerium für Wissenschaft und Kultur (MWK) Niedersachsen and the Volkswagenstiftung under grant INST 186/901-1 to build parts of the experimental apparatus. A.M.W. and A.K. also acknowledge the Max Planck Society for the Advancement of Science. I.R. and A.M.W. acknowledge support from the Niedersächsisch-Israelische Gemeinschaftsvorhaben under project 574 7 022. T.N.K. acknowledges the European Research Council (ERC) under the European Union's Horizon 2020 research and innovation program (grant agreement 833404). D.B. thanks the BENCh graduate school, funded by the DFG (389479699/GRK2455). M.H. and H.G. acknowledge support from the National Science Foundation (grant CHE-1462109). H.G. also acknowledges the Alexander von Humboldt Foundation for a Humboldt Research Award. **Author contributions:** D.B., I.R., P.R.S., D.J.A., and A.K. developed the PAC kinetic model and carried out the analysis. I.R. and D.B. wrote the supplementary materials. I.R. and P.R.S. performed experiments that led to the data presented in this work. M.H. and H.G. performed the theoretical calculations and analyzed the results. T.Z. and D.S. carried out TPD measurements that were essential to the application of the PAC model. D.S. and T.N.K. participated in discussion of the results, analysis, data interpretation, and revisions. D.J.A. had major conceptual contributions to data interpretation and supplementary materials and manuscript revisions. A.M.W. wrote the manuscript and participated in revisions. All authors provided critical input to the writing of the paper. **Competing interests:** None declared. **Data and materials availability:** There are no restrictions on materials used in this work. All data needed to evaluate the conclusions in the paper are present in the paper or the supplementary materials and are publicly available in the repository (*22*).

SUPPLEMENTARY MATERIALS

science.sciencemag.org/content/369/6510/1461/suppl/DC1
Materials and Methods
Supplementary Text
Figs. S1 to S13
Tables S1 to S4
References (*23*–*41*)

24 May 2020; accepted 14 July 2020
10.1126/science.abc9581

Following the microscopic pathway to adsorption through chemisorption and physisorption wells

Dmitriy Borodin, Igor Rahinov, Pranav R. Shirhatti, Meng Huang, Alexander Kandratsenka, Daniel J. Auerbach, Tianli Zhong, Hua Guo, Dirk Schwarzer, Theofanis N. Kitsopoulos and Alec M. Wodtke

Science **369** (6510), 1461-1465.
DOI: 10.1126/science.abc9581

Nature of the molecule-surface encounter

Adsorption is an important initial step in all heterogeneous chemical processes. However, detailed adsorption dynamics are complex and challenging to follow experimentally. Using the fact that vibrationally excited carbon monoxide molecules can be trapped on the Au(111) surface with all degrees of freedom being equilibrated except the vibrational ones, Borodin *et al.* show that the vibrational relaxation time can serve as an internal clock to follow the microscopic pathways of adsorption and equilibration on the surface. On the basis of molecular beam experiments and theoretical modeling of this prototypical system, the authors reveal the intricate interplay between physisorption and chemisorption states. These observed characteristics are relevant to many other heterogeneous systems.

Science, this issue p. 1461